Mechanical Properties of Thermally Annealed Cu/Ni and Cu/Al Multilayer Thin Films: Solid Solution vs Intermetallic Strengthening

Yang Zhou , Catherine Chun , Junlan Wang *

Posted Date: 3 January 2024

doi: 10.20944/preprints202401.0083.v1

Keywords: metallic multilayer; Cu/Ni; Cu/Al; thermal strengthening; intermetallic strengthening

Article

Mechanical Properties of Thermally Annealed Cu/Ni and Cu/Al Multilayer Thin Films: Solid Solution vs Intermetallic Strengthening

Yang Zhou, Katherine Chun and Junlan Wang *

Department of Mechanical Engineering, University of Washington, Seattle, WA 98195
* Correspondence: Corresponding author: Prof. J. Wang, junlan@u.washington.edu.

Abstract: In this study, Cu/Ni and Cu/Al multilayer thin films with individual layer thickness varying from 25 nm to 200 nm were deposited at room temperature and further annealed up to 300 ℃. The mechanical and microstructural properties of the multilayers were characterized by nanoindentation, x-ray diffraction, and scanning electron microscopy. Both systems exhibited an increase in hardness with increasing annealing temperature. However, the Cu/Ni system showed a gradual and moderate (up to 30%) hardness increase from room temperature to 300 ℃, while the Cu/Al system showed a sharp increase (~150%) between 125℃ and 200℃. This distinct strengthening behavior is attributed to solid solution formation in Cu/Ni and diffusion-activated intermetallic formation in Cu/Al.

Keywords: metallic multilayer; Cu/Ni; Cu/Al; thermal strengthening; intermetallic strengthening

1. Introduction

Metallic multilayers are thin films and coatings consisting of alternating layers of two of more different metals. Compared with their bulk counterparts, metallic multilayers offer some extraordinary properties such as mechanical strength, wear and corrosion resistance, and thermal stability [1-5]. The superior mechanical strength in metallic multilayers have been attributed to multiple factors such as layer thickness [6], interface structure [7], and thermal annealing conditions [8, 9].

The number of interfaces and the corresponding layer thickness can affect the metallic multilayer strength by controlling the dislocation motions. For multilayers with individual layer thickness of 50 nm and greater, strengthening occurs by dislocation pile-up at the layer interfaces which can be explained by the Hall-Petch relation [10-13]. When the layer thickness is between 10 and 50 nm, due to strong repulsion among like-sign coplanar dislocations, the multilayer strengthening can be explained by confined layer slip (CLS) [14-17], involving the movement of a single dislocation loop parallel to the interface within individual layers. The multilayer strength approaches the theoretical value when the layer thickness is around 5 nm. At this thickness scale, the strength of multilayers is affected by coherency stress, misfit dislocations, moduli differences, texture, and chemical intermixing along the interface [10, 13]. The peak strength is determined by the stress needed to transmit a single dislocation across the interface.

In addition to the layer thickness, the crystallography of layers also affects the multilayer strength. For two materials sharing the same crystal structure, such as Cu/Ni multilayers, the strengthening mechanism can be ascribed to the coherency stress at the interfaces [18, 19]. For multilayer systems which are composed of different crystal structures, such as Cu/Nb multilayers, the different crystal structures at two sides of the interface may lead to discontinuity of slip system and different slip vectors. The flow strength is determined by the transmission of dislocation from one material to another [20, 21]. However, the original crystal structure of the individual material may be changed when the layer thickness is small enough. For example, in Ag/Fe multilayers, phase transformation in Fe from BCC to FCC occurs when the layer thickness reaches 5 nm [22]. Also, a

 doi:10.20944/preprints202401.0083.v1

superlattice structure has been observed in Cu/Ni multilayer thin films when the layer thickness is smaller than 5 nm [23].

In addition to the aforementioned mechanisms, mechanical properties of multilayer thin films can be affected by heat treatment as well. Annealed Ti/Ni multilayer thin films experience enhanced hardness with increasing annealing temperature [8, 9]. At low annealing temperatures, the increase in hardness can be explained by grain boundary relaxation. At high annealing temperatures, the hardness increase is mainly attributed to the formation of alloys. In some special metallic multilayer systems, such as Cu/Al, the negative enthalpy activates the spontaneous formation of intermetallic phases in as-deposited and annealed samples [24, 25].

Motivated by the unique advantages of metallic multilayers, and the thermal-mechanical strengthening mechanisms discovered so far, two model multilayer systems, Cu/Ni and Cu/Al, are studied in this work. One key benefit of selecting the Cu/Ni and Cu/Al multilayer systems is that Cu-Ni and Cu-Al have interesting and distinctly different phase diagrams. Cu-Ni is a simple isomorphous system with a suggested spinodal decomposition of the FCC phase below 350°C [26]. The up to 100% mutual solubility of Cu and Ni provides a wide composition range for studying their intermixing effect on the mechanical properties of the resulting alloys. The Cu-Al system is very different. Although Al is intrinsically a soft and ductile metal, it is known to form several different intermetallic phases with Cu when mixed at different atomic ratios. Just in the low-temperature range between 150° and 300°C, there are several different Cu-Al intermetallic compounds, e.g., γ_2 phase (Cu_9Al_4): 69.2 atm% Cu, δ phase (Cu_3Al_2 / Al_2Cu_3): 60.0 atm% Cu, ζ_2 phase (Cu_4Al_3): 57.1 atm% Cu, η_2 phase (CuAl): 50.0 atm% Cu, and θ phase ($CuAl_2$): 33.3 atm% Cu [27]. The rich intermetallic phases in Cu-Al make the thermally annealed Cu-Al a much more interesting and potentially stronger alloy than the annealed Cu-Ni, thus could significantly enhance the strength of the Cu/Al multilayer system.

Existing studies in Cu/Ni multilayers attributed the strengthening mechanisms to the layer thickness effect and the coherency stress at interfaces [7, 16, 23, 28, 29]. On the other hand, the hardness of Cu/Al multilayers not only follows the layer thickness effect but also is affected by the formation of intermetallic phases [25, 30]. The comparative study on thermally-annealed Cu/Ni and Cu/Al multilayers in this work will shed light on the different thermal strengthening mechanisms of these two metallic multilayer systems.

2. Experimental Details

Cu/Ni and Cu/Al multilayers were prepared with an Orion 5 UHV magnetron sputtering system (AJA International, Inc., MA), under a base vacuum of ~ 1×10^{-8} mbar. Single crystal (100) Si wafer was used as the substrate for all samples. Cu (99.995%), Ni (99.995%) and Al (99.999%) targets were used to deposit the two multilayer systems by DC sputtering, The deposition power was 100W and background Ar pressure was 2 mTorr. A thin titanium layer (~10 nm) deposited from a Ti (99.995%) target was used as a bonding layer between the Cu/Ni multilayers and the substrate. Without the adhesion layer, the Cu/Ni multilayers tend to automatically delaminate from the substrate [31]. The range of individual layer thicknesses, h, was from 25 nm to 200 nm for the Cu/Ni and 25 nm to 100 nm for Cu/Al, while the thickness ratio between Cu and Ni (Al) was held at 1:1. Total thickness varied from 1 to 2 μm. For comparison purposes, 500 nm thick Cu-Ni and Cu-Al co-sputtered samples were also prepared by matching up the deposition power of Ni and Al to Cu in order to obtain a nominal 1:1 atomic ratio between the two elements. After deposition, selected samples were vacuum annealed for 2 hours using a muffle furnace (Lindberg Blue M, Thermo Scientific, NC) at temperatures varying from 100℃ to 300℃.

Following the sample preparation, a Ubi1 Nanomechanical Test Instrument (Hysitron, Inc., MN) with a Berkovich indenter tip was used to characterize the hardness of both as-deposited and annealed samples. A load function with 10s loading, 5s holding, and 10s unloading was used for all the testing. The depth of indentation was controlled below 15% of the total film thickness to avoid substrate effect. The hardness was calculated by dividing the maximum load by the contact area

Preprints (www.preprints.org) | NOT PEER-REVIEWED | Posted: 3 January 2024 doi:10.20944/preprints202401.0083.v1

following the standard Oliver and Pharr method [32]. At least 60 indentations were carried out on each sample at varying loads to ensure repeatability of results.

The crystallinity of both as-deposited and annealed multilayers were studied by x-ray diffraction (XRD) using a Bruker D8 Discover with Cu Kα radiation. The angle was scanned from 15° to 90°, with the scan time of 90 seconds per frame. Sample surface and cross-section morphologies were characterized by scanning electron microscopy on a FEI Sirion XL30.

3. Results and Discussions

3.1. SEM Morphology of As-deposited Samples

Cross-sectional morphologies of three as-deposited Cu/Ni multilayer samples (layer thicknesses of 200, 100 and 25 nm, respectively) and one co-sputtered Cu-Ni sample are shown in Figure 1. Highly textured layer-by-layer structures can be found in the multilayer samples. The 200 nm and 100 nm layer thickness samples display clear columnar structures in the Ni layers. Columnar structure is not obvious in the 25 nm sample due to small layer thickness. Grain structure is not clear in the Cu layers due to the ductile deformation of the layers during fracture. The entire co-sputtered Cu-Ni film shows a columnar structure.

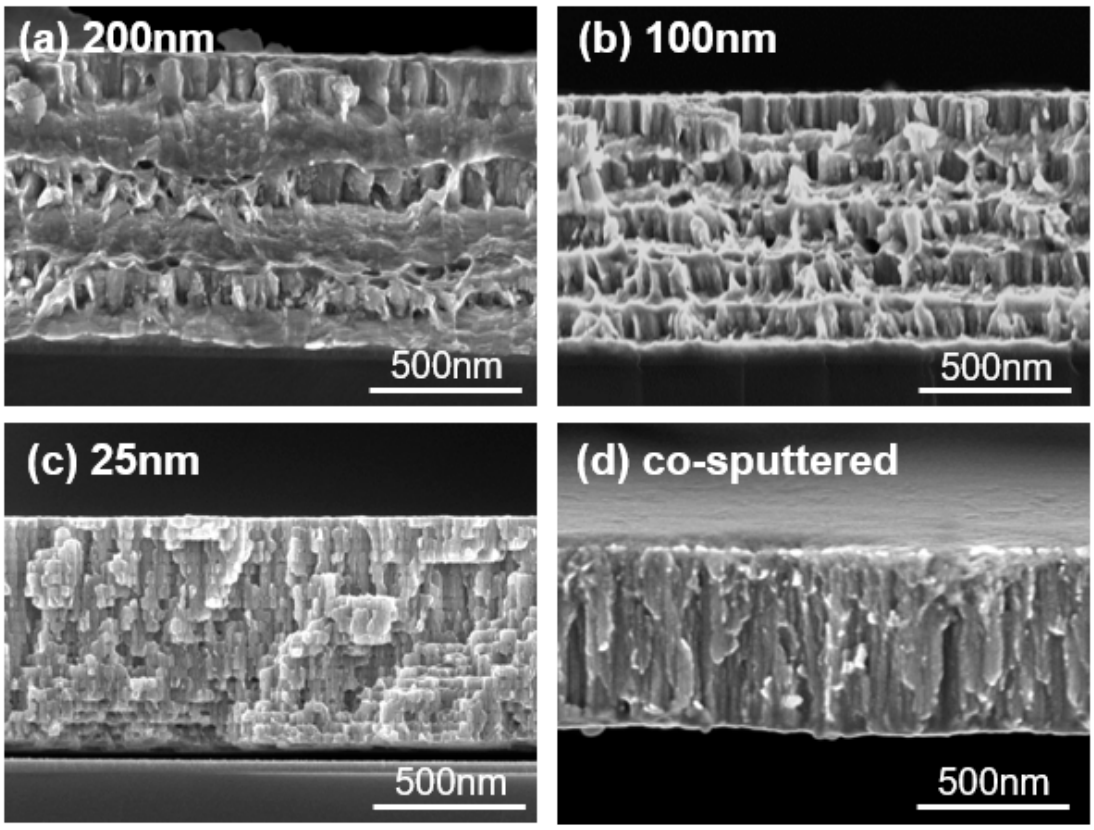

Figure 1. Cross-sectional SEM images for as-deposited Cu/Ni samples with layer thickness of: (a) 200 nm, (b) 100 nm, and (c) 25 nm as well as a co-sputtered Cu-Ni sample (d).

Cross-sectional morphologies for three as-deposited Cu/Al samples, with layer thickness from 100 down to 25 nm, and one co-sputtered Cu-Al sample are shown in Figure 2. The multilayer samples show well-defined layer-by-layer structures. However, the high ductility of both the Cu and Al layers led to significant plastic deformation when the samples were fractured for cross-sectional imaging, which makes the microstructure undiscernible. The Cu-Al co-sputtered sample portrays another clear columnar structure.

Preprints (www.preprints.org) | NOT PEER-REVIEWED | Posted: 3 January 2024 doi:10.20944/preprints202401.0083.v1

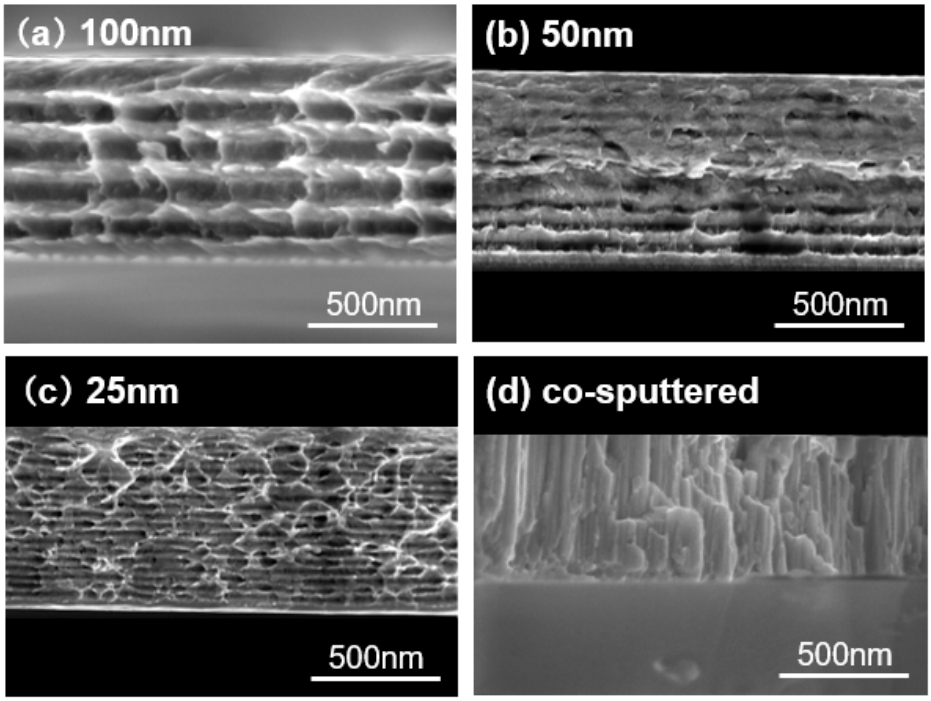

Figure 2. Cross-sectional SEM images for as-deposited Cu/Al multilayer samples with layer thickness of: (a) 100 nm, (b) 50 nm and (c) 25 nm, as well as a co-sputtered Cu-Al sample (d).

3.2. Hardness

Hardness is determined by nanoindentation and is plotted as a function of annealing temperature for Cu/Ni and Cu/Al multilayers and co-sputtered samples in Figure 3. In both plots, there is an obvious increase in hardness with decreasing layer thickness in as-deposited samples, similar to those observed in the literature due to layer interface strengthening [7]. Increasing hardness with increasing annealing temperature was demonstrated in both Cu/Ni and Cu/Al systems, however, with a significantly different trend and amount. Co-sputtered samples showed higher hardness than all the multilayer samples in the entire temperature range for both systems.

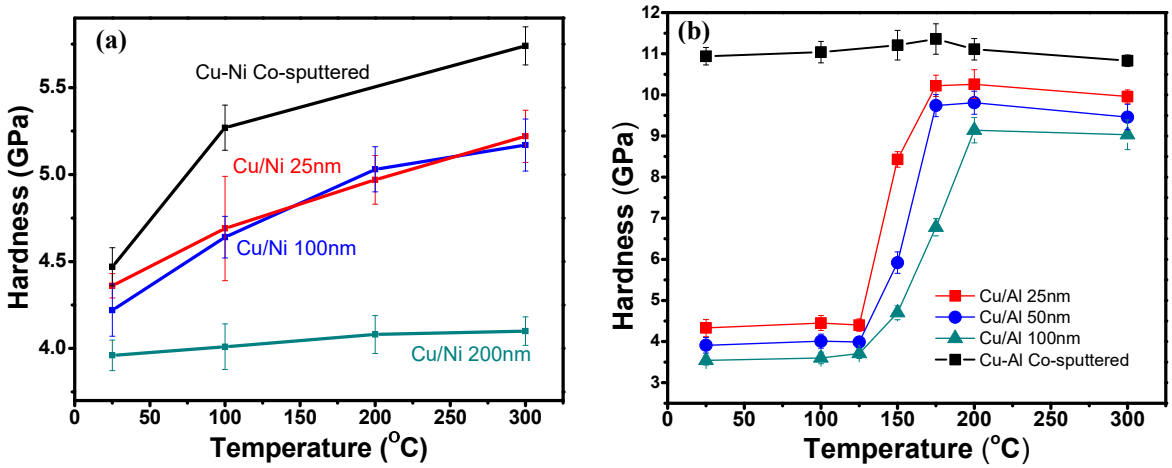

Figure 3. The hardness of (a) Cu/Ni multilayer and co-sputtered Cu-Ni, (b) Cu/Al multilayer and co-sputtered Cu-Al thin films with different annealing temperatures and different layer thicknesses.

As shown in Figure 3a, Cu/Ni samples display continuous and slow hardness increase from the as-deposited sample to the 300℃ annealed sample. Even at the highest annealing temperature of 300 ℃, the increase in hardness is still moderate (<30%) with respect to the as-deposited case. More strengthening was observed for the thinner layers (e.g., 25 and 100 nm) and co-sputtered samples.

Preprints (www.preprints.org) | NOT PEER-REVIEWED | Posted: 3 January 2024 doi:10.20944/preprints202401.0083.v1

Meanwhile, as shown in Figure 3b, Cu/Al samples show a dramatic increase in hardness (~150%) within a narrow temperature range - 125℃ to 175 ℃ for the 25 and 50 nm layer thickness, and 125 ℃ to 200 ℃ for the 100 nm layer thickness. However, for temperatures below 125℃, the multilayer showed no visible changes in hardness with respect to temperature. The multilayer hardness leveled off after 175 ℃ for the 25 and 50 nm layer thickness samples, and after 200 ℃ for the 100 nm layer thickness sample. The hardness of the co-sputtered Cu-Al sample remained at high and constant values around ~11 GPa, throughout the entire temperature range. This behavior is totally different from that of the co-sputtered Cu-Ni, which increased with annealing temperature.

3.3. XRD Spectra

XRD spectra of as-deposited Cu/Ni multilayers and co-sputtered Cu-Ni thin film samples are shown in Figure 4a. Both Cu and Ni show an FCC structure with strong peaks for Cu (111), Ni (111), Cu (200), and Ni (200). Comparisons of the XRD plots between different layer thicknesses reveal that the distance between Cu (111) and Ni (111) peaks in the 25 nm layer thickness sample is slightly smaller than those of the other two samples. The decreased peak distance is probably due to distortion of the lattice at each layer interface. The larger number of interfaces in the 25 nm layer thickness sample are expected to result in a higher amount of distortion and subsequent residual stress. Previous work showed that as the layer thickness reduced from 100 nm to 25 nm, the residual stress in the Ni layers increased from 0.88 GPa to 1.45 GPa [31]. For the Cu-Ni co-sputtered sample, the Cu and Ni peaks - Cu (111) and Ni (111), and Cu (200) and Ni (200) – merge between their original positions in the thicker layers, indicating a new FCC structure with a lattice constant in between those of Cu and Ni.

Figure 4b demonstrates the XRD spectra of the 100 nm layer thickness Cu/Ni samples at different annealing temperatures. Comparison of XRD patterns between the as-deposited and annealed samples show no obvious change regardless of the annealing temperatures. Although not included, XRD spectra of the 200 nm and 25nm layer thickness samples show similar behavior – no clear temperature dependence.

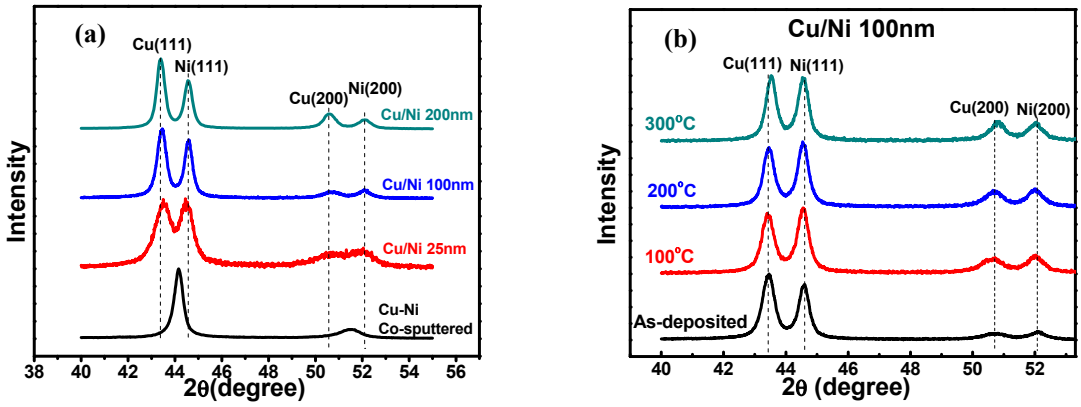

Figure 4. XRD spectra for Cu/Ni multilayer samples: (a) as-deposited multilayers with different layer thickness (including co-sputtered), and (b) 100 nm layer thickness samples at different annealing temperature.

XRD spectra of the Cu/Al samples are shown in Figure 5. In as-deposited Cu/Al multilayer samples, shown in Figure 5(a), there is an obvious separation between the Cu (111) and Al (111) peaks. However, in the co-sputtered Cu-Al sample, the two metal elements form intermetallic Al_2Cu_3 phases, resulting in a completely different XRD spectrum. The peaks near 44 degree is likely a combination of a Cu (111) and the Al_2Cu_3 (102) peaks.

Preprints (www.preprints.org) | NOT PEER-REVIEWED | Posted: 3 January 2024 doi:10.20944/preprints202401.0083.v1

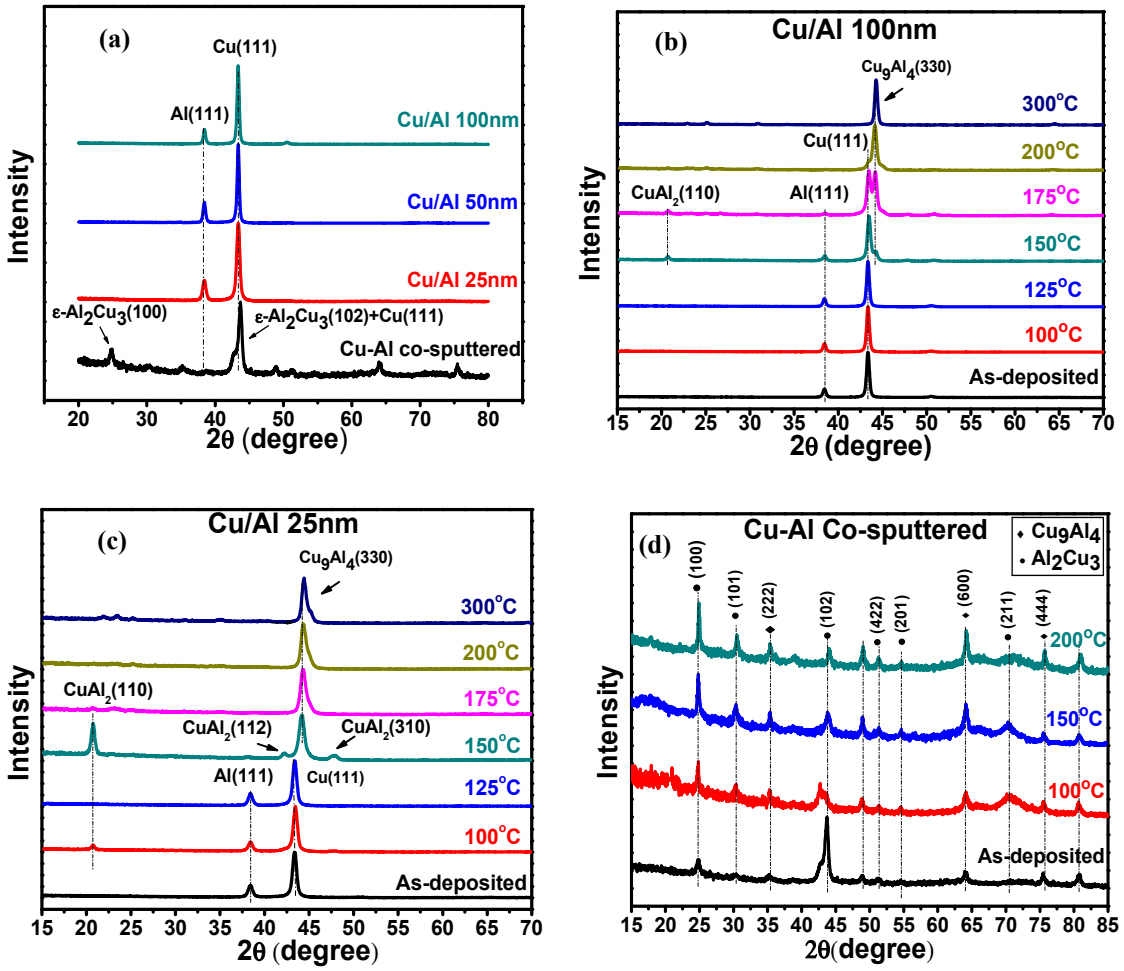

Figure 5. XRD spectra for Cu/Al thin films: (a) as-deposited of different layer thickness (including the co-sputtered); as-deposited and annealed samples: (b) individual layer thickness of 100 nm, (c) individual layer thickness of 25 nm, (d) co-sputtered Cu-Al.

In Figure 5b and c, the XRD spectra of the 100 and 25 nm layer thickness samples demonstrate that below 150 ℃, there is no discernible peak change between the as-deposited and the low temperature annealed (100 ℃ and 125 ℃), and the Cu (111) and Al (111) peaks remained stable. This explains why the hardness shown in Figure 3b remained constant at these temperatures. However, intermetallic Cu-Al phases started to appear at higher annealing temperatures. For the 100 nm layer thickness sample, two different intermetallic peaks are differentiated at 150 ℃ - $CuAl_2$ (110) and Cu_9Al_4 (330). The Cu_9Al_4 (330) peak becomes more prominent at 175 ℃, and dominant after 200 ℃. At higher annealing temperatures, Cu (111) and $CuAl_2$ (110) peaks are no longer present. It is known that the diffusivity of Cu in Al is greater than that of Al in Cu, therefore $CuAl_2$ phase is first formed when Cu is saturated in Al [24, 33]. At even higher temperatures (~175℃), the Cu + $CuAl_2$ → Cu_9Al_4 reaction happens at the interfaces; a similar reaction happens in the Cu/Al 25 nm sample as well (Figure 5c). However, intermetallic formation occurs at lower annealing temperature (100 ℃) phases in the 25 nm samples than that in the 100 nm samples, indicating faster diffusion of atoms in thinner layers even at a lower annealing temperature. In the co-sputtered Cu-Al thin film, Cu_9Al_4 and ε-Al_2Cu_3 phases are found in both as-deposited and after annealing (shown in **Figure 5**(d)). The largest difference between multilayered and co-sputtered Cu/Al samples are the rich intermetallic phases present in the as-deposited as well as thermally annealed co-sputtered sample.

XRD analysis also supports the principle of post-deposition annealing strengthening, since the intermetallic phases ($CuAl_2$ and Cu_9Al_4) are much harder than pure Cu and Al. The smaller layer thicknesses of the 50 nm and 25 nm Cu/Al samples, in comparison to the 100 nm Cu/Al sample,

Preprints (www.preprints.org) | NOT PEER-REVIEWED | Posted: 3 January 2024 doi:10.20944/preprints202401.0083.v1

promotes diffusion and thus faster increase and saturated hardness. Cu-Al co-sputtered samples have sufficient mixing of Cu and Al during the deposition process, forming intermetallic phases even at room temperature and maintaining the intermetallic structure and hardness after annealing.

3.4. SEM Morphology of Annealed Samples

Annealed samples show different cross-sectional morphologies from as-deposited samples. Figure 6 shows the cross-sectional SEM images of the 100 nm layer thickness Cu/Ni as-deposited sample and those annealed at 100℃, 200 ℃, and 300℃, respectively. The as-deposited sample shows clear layer-by-layer structure. Nevertheless, in samples annealed at higher temperatures, the Cu layer appears much thicker than in the as-deposited case. This phenomenon is especially pronounced in the 300℃ annealed sample. Therefore, higher annealing temperatures promote diffusion between Cu and Ni layers.

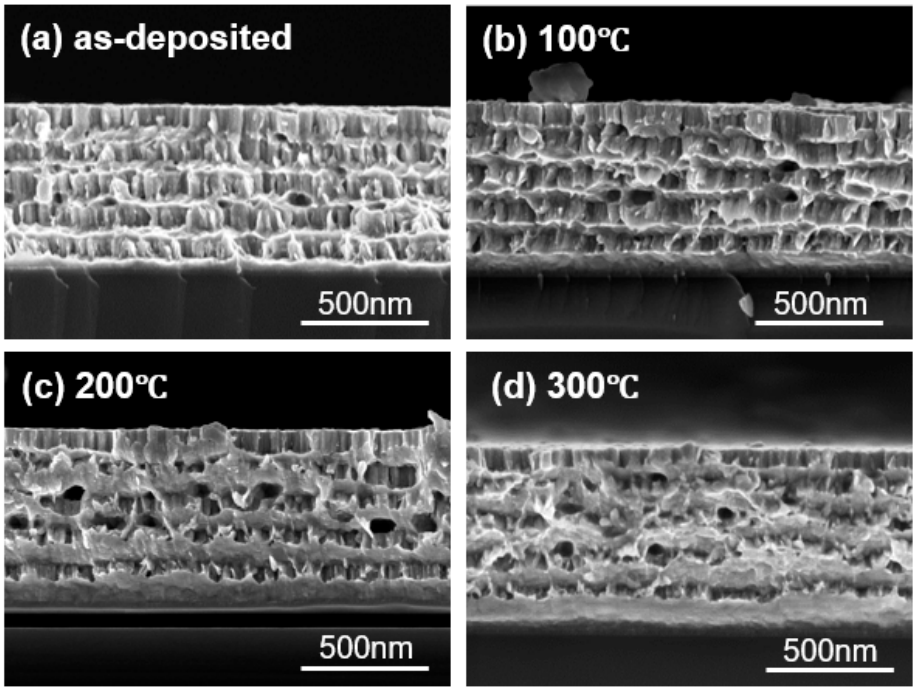

Figure 6. Cross-sectional SEM images for Cu/Ni 100 nm samples: (a) as-deposited, (b) 100℃ annealed, (c) 200℃ annealed, and (d) 300℃ annealed.

At low annealing temperatures (<100℃), no obvious diffusion is shown in cross-sectional SEM (Fig. 6b). Therefore, the improved mechanical properties may be attributed to grain boundary relaxation [8, 34, 35]. Annealing increases grain boundary's transition to a more ordered equilibrium state, blocking the movement of dislocations thus enhancing hardness. At high annealing temperatures (greater than 100℃), diffusion and solid solution formation lead to deformation and presence of stress fields in the samples, which may be the mechanism of enhancement in the Cu/Ni multilayer thin film at high annealing temperatures.

Figure 7 shows the cross-sectional images of the Cu/Al 100 nm sample with different annealing temperatures, from 125℃ to 300℃. The first two images show a clear layer-by-layer structure without any obvious difference, validating the XRD-based conclusion that little diffusion occurs at annealing temperatures lower than 150℃ in Cu/Al 100 nm samples. The as-deposited and 125℃ samples show undulating structures, which may be due to the ductility of Cu and Al during fracture. The images of Cu/Al annealed at 150℃ and 175℃ show thinner Cu layers due to diffusion. At annealing temperatures of 200℃ and 300℃, the Cu and Al layers become increasingly intermixed, explaining the different XRD peaks between 300℃ annealed samples and as-deposited ones. Furthermore, the fractal cross-sections in Figure 7(c-f) appear visibly and increasingly smoother, providing further evidence of the brittle intermetallic phase formation with increasing temperature.

Preprints (www.preprints.org) | NOT PEER-REVIEWED | Posted: 3 January 2024 doi:10.20944/preprints202401.0083.v1

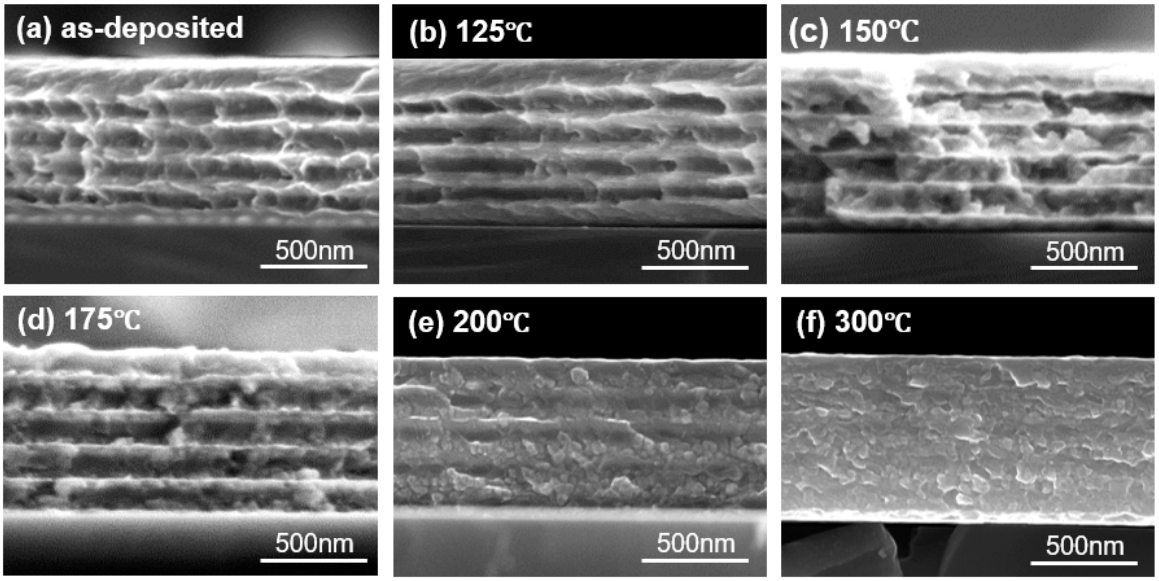

Figure 7. Cross-sectional SEM images for Cu/Al 100 nm samples: (a) as-deposited, and (b) 125℃, (c) 150℃, (d) 175℃ , (e) 200℃, (f) 300℃ annealed.

4. Conclusions

In this work, the thermal-annealing induced strengthening was investigated in Cu/Ni and Cu/Al multilayer systems with individual layer thickness ranging between 25 nm and 200 nm. The Cu/Ni samples showed a gradual and slow hardness increase, up to 30%, from room temperature to 300 ℃. Meanwhile, Cu/Al samples experienced a dramatic hardness increase, around 150%, over a narrow range of annealing temperature between 125 ℃ and 200 ℃. At annealing temperature below 125 ℃ or higher than 200 ℃, the hardness of Cu/Al samples showed little temperature dependence. The co-sputtered Cu-Ni and Cu-Al samples showed higher hardness than the corresponding multilayered samples, although with distinctly different temperature dependence – Cu-Ni hardness increased with annealing temperature while Cu-Al stayed constant high throughout the entire temperature range.

In Cu/Ni samples, increased hardness with decreasing layer thickness in as-deposited samples confirmed the layer thicknesses effect in metallic multilayers. Neither the XRD spectra nor the cross-sectional SEM demonstrated obvious structure difference between low-temperature annealed and as-deposited samples in Cu/Ni multilayers. However, diffusion became observable at an annealing temperature of 200℃. Diffusion of Cu and Ni layers at high-temperatures also contributed to the increased hardness, through the formation of solid solutions. Strengthening in low-temperature annealed samples may be attributed to grain boundary relaxation.

In Cu/Al multilayer samples, annealed samples experienced an enormous hardness increase between 125℃ and 200℃. From XRD and cross-sectional SEM results, annealing promoted Cu diffusion into the adjacent Al layers to form various intermetallic phases. These intermetallic phases ($CuAl_2$ and Cu_9Al_4) led to a drastic increase in hardness in Cu/Al samples. Meanwhile, due to the rich intermetallic phases already existing in the as-deposited Cu-Al co-sputtered samples, the hardness reached ~11 GPa in the as-deposited state and remained constant after annealing. Thus, the hardness of co-sputtered Cu-Al samples may be regarded as an asymptotic value for annealed Cu/Al multilayer systems.

The results of this study highlighted two different thermal strengthening mechanisms between the two metallic multilayers systems: solid solutions formation in Cu/Ni and intermetallic phases in Cu/Al. The improved understanding of these strengthening mechanisms can provide guidelines for future design and application of engineered multilayer materials.

Acknowledgments: The authors acknowledge the financial support by the University of Washington Royal Research Fund (grant no. 68-2003). Part of this work was conducted at the University of Washington Molecular

Analysis Facility, which is supported in part by funds from the Molecular Engineering & Sciences Institute, the Clean Energy Institute, and the National Science Foundation (NNCI-2025489 and NNCI-1542101).

References

1. Tench, D. and J. White, *Enhanced tensile strength for electrodeposited nickel-copper multilayer composites.* Metallurgical and Materials Transactions A, 1984. **15**(11): p. 2039-2040.
2. Embury, J. and J. Hirth, *On dislocation storage and the mechanical response of fine scale microstructures.* Acta Metallurgica et Materialia, 1994. **42**(6): p. 2051-2056.
3. Troyon, M. and L. Wang, *Influence of saccharin on the structure and corrosion resistance of electrodeposited CuNi multilayers.* Applied surface science, 1996. **103**(4): p. 517-523.
4. Nabiyouni, G. and W. Schwarzacher, *Growth, characterization and magnetoresistive study of electrodeposited Ni/Cu and Co–Ni/Cu multilayers.* Journal of crystal Growth, 2005. **275**(1): p. e1259-e1262.
5. Misra, A. and R. Hoagland, *Plastic flow stability of metallic nanolaminate composites.* Journal of materials science, 2007. **42**(5): p. 1765-1771.
6. Wang, J. and A. Misra, *An overview of interface-dominated deformation mechanisms in metallic multilayers.* Current Opinion in Solid State and Materials Science, 2011. **15**(1): p. 20-28.
7. Wang, J., Q. Zhou, S. Shao, and A. Misra, *Strength and plasticity of nanolaminated materials.* Materials Research Letters, 2016. **5**(1): p. 1-19.
8. Yang, Z. and J. Wang, *Orientation-Dependent Hardness in As-Deposited and Low-Temperature Annealed Ti/Ni Multilayer Thin Films.* Journal of Applied Mechanics, 2015. **82**(1): p. 011008-011008.
9. Yang, Z. and J. Wang, *Coupled annealing temperature and layer thickness effect on strengthening mechanism of Ti/Ni multilayer thin films.* Journal of the Mechanics and Physics of Solids, 2016. **88**: p. 72-82.
10. Wang, J. and A. Misra, *An overview of interface-dominated deformation mechanisms in metallic multilayers.* Current Opinion in Solid State & Materials Science, 2011. **15**(1): p. 20-28.
11. Friedman, L.H., *Exponent for Hall-Petch behaviour of ultra-hard multilayers.* Philosophical Magazine, 2006. **86**(11): p. 1443-1481.
12. Kaneko, Y., Y. Mizuta, Y. Nishijima, and S. Hashimoto, *Vickers hardness and deformation of Ni/Cu nano-multilayers electrodeposited on copper substrates.* Journal of Materials Science, 2005. **40**(12): p. 3231-3236.
13. Misra, A., J.P. Hirth, and H. Kung, *Single-dislocation-based strengthening mechanisms in nanoscale metallic multilayers.* Philosophical Magazine a-Physics of Condensed Matter Structure Defects and Mechanical Properties, 2002. **82**(16): p. 2935-2951.
14. Li, Q. and P.M. Anderson, *Dislocation-based modeling of the mechanical behavior of epitaxial metallic multilayer thin films.* Acta materialia, 2005. **53**(4): p. 1121-1134.
15. Rao, S.I. and P.M. Hazzledine, *Atomistic simulations of dislocation-interface interactions in the Cu-Ni multilayer system.* Philosophical Magazine a-Physics of Condensed Matter Structure Defects and Mechanical Properties, 2000. **80**(9): p. 2011-2040.
16. Anderson, P.M. and J.S. Carpenter, *Estimates of interfacial properties in Cu/Ni multilayer thin films using hardness data.* Scripta Materialia, 2010. **62**(6): p. 325-328.
17. Yang, M., J. Xu, H. Song, and Y. Zhang, *Effects of tilt interface boundary on mechanical properties of Cu/Ni nanoscale metallic multilayer composites.* Chinese Physics B, 2015. **24**(9).
18. Hoagland, R.G., T.E. Mitchell, J.P. Hirth, and H. Kung, *On the strengthening effects of interfaces in multilayer fcc metallic composites.* Philosophical Magazine a-Physics of Condensed Matter Structure Defects and Mechanical Properties, 2002. **82**(4): p. 643-664.

19. Hoagland, R.G., R.J. Kurtz, and C.H. Henager, *Slip resistance of interfaces and the strength of metallic multilayer composites.* Scripta Materialia, 2004. **50**(6): p. 775-779.
20. Wang, J., R.G. Hoagland, and A. Misra, *Mechanics of nanoscale metallic multilayers: From atomic-scale to micro-scale.* Scripta Materialia, 2009. **60**(12): p. 1067-1072.
21. Wang, J., R.G. Hoagland, J.P. Hirth, and A. Misra, *Atomistic modeling of the interaction of glide dislocations with "weak" interfaces.* Acta Materialia, 2008. **56**(19): p. 5685-5693.
22. Li, J., Y. Chen, S. Xue, H. Wang, and X. Zhang, *Comparison of size dependent strengthening mechanisms in Ag/Fe and Ag/Ni multilayers.* Acta Materialia, 2016. **114**: p. 154-163.
23. Liu, Y., D. Bufford, H. Wang, C. Sun, and X. Zhang, *Mechanical properties of highly textured Cu/Ni multilayers.* Acta Materialia, 2011. **59**(5): p. 1924-1933.
24. JIANG, H., J. DAI, H. TONG, B. DING, Q. SONG, and Z. HU, *INTERFACIAL REACTIONS ON ANNEALING CU/AL MULTILAYER THIN-FILMS.* Journal of Applied Physics, 1993. **74**(10): p. 6165-6169.
25. Zhou, Q., S. Li, P. Huang, K.W. Xu, F. Wang, and T.J. Lu, *Strengthening mechanism of super-hard nanoscale Cu/Al multilayers with negative enthalpy of mixing.* Apl Materials, 2016. **4**(9).
26. Gupta, K.P., *The Cu-Ni-Ti(Copper-Nickel-Titanium) system.* Journal of Phase Equilibria, 2002. **23**(6): p. 541-547.
27. Massalski, T.B. and H. Okamoto, *Binary Alloy Phase Diagrams*, 1990, ASM International, Materials Park, Ohio.
28. Barshilia, H.C. and K.S. Rajam, *Characterization of Cu/Ni multilayer coatings by nanoindentation and atomic force microscopy.* Surface & Coatings Technology, 2002. **155**(2-3): p. 195-202.
29. Zhu, X.Y., X.J. Liu, R.L. Zong, F. Zeng, and F. Pan, *Microstructure and mechanical properties of nanoscale Cu/Ni multilayers.* Materials Science and Engineering a-Structural Materials Properties Microstructure and Processing, 2010. **527**(4-5): p. 1243-1248.
30. Ito, T., R. Yamamoto, and A. Yoshihara, *Mechanical-Properties of Cu/Al Multilayered Thin-Films.* Surface & Coatings Technology, 1991. **45**(1-3): p. 215-220.
31. McDonald, I.G., W.M. Moehlenkamp, D. Arola, and J. Wang, *Residual stresses in Cu/Ni Multilayer thin films measured using the $\sin^2\psi$ method.* Experimental Mechanics, 2018. **(In Press) DOI : 10.1007/s11340-018-00447-2**.
32. Oliver, G.M.P.a.W.C., *Measurement of Thin Film Mechanical Properties Using Nanoindentation.* 1992.
33. M. Honarpisheh, M.A., M. Sedighi, *Investigation of annealing treatment on the interfacial properties of explosive-welded Al_Cu_Al multilayer.* 2012.
34. Ning, T., Q.L. Yu, and Y.Y. Ye, *Multilayer Relaxation at the Surface of Fcc Metals - Cu, Ag, Au, Ni, Pd, Pt, Al.* Surface Science, 1988. **206**(1-2): p. L857-L863.
35. Rodriguez, A.M., G. Bozzolo, and J. Ferrante, *Multilayer Relaxation and Surface Energies of Fcc and Bcc Metals Using Equivalent Crystal Theory.* Surface Science, 1993. **289**(1-2): p. 100-126.